

Synthesis and Solution Properties of an Associative Polymer with Excellent Salt-Thickening

Chuanrong Zhong,¹ Wei Wang,^{1,2} Mingming Yang¹

¹State Key Laboratory of Oil and Gas Reservoir Geology and Exploitation, Chengdu University of Technology, Chengdu 610059, Sichuan, China

²Oil Production Technology Research Institute, PetroChina Dagang Oilfield Limited Company, Tianjin 300280, China

Received 15 January 2011; accepted 5 January 2012

DOI 10.1002/app.36743

Published online in Wiley Online Library (wileyonlinelibrary.com).

ABSTRACT: To enhance apparent viscosities in brine solutions with high salinities for associative water-soluble polymers, a novel macromonomer (APEO): allyl-capped octylphenoxy poly(ethylene oxide) (degree of polymerization: 14) was synthesized, and a novel tetra-polymer (PAVO) was synthesized by copolymerizing APEO, acrylamide (AM), sodium 2-acrylamido-2-methylpropane sulfonate (NaAMPS), and vinyl biphenyl (VP). The macromonomer and the PAVO polymer were characterized with Fourier transform infrared (FTIR) spectroscopy and proton nuclear magnetic resonance (¹H-NMR). The apparent viscosities of PAVO in pure water were very low over all polymer concentrations, and the critical association concentration (C_p^*) was 0.15 g dL⁻¹. However, in brine solutions above 40 g L⁻¹ NaCl or 10 g L⁻¹ CaCl₂, the intermolecular hydrophobic

associations of octylphenyl groups and biphenyl groups were enhanced dramatically, the polymer chains were still comparatively extended due to the incorporation of APEO into the polymer, C_p^* was reduced to 0.10 g dL⁻¹, and the apparent viscosities were significantly higher than in pure water. The PAVO brine solutions exhibited excellent salt-thickening induced by metallic univalent or bivalent cations, heat-thickening effect, shear-thickening behavior, and thixotropy. Moreover, the brine solution also performed good resistance to ageing because of the simultaneous incorporation of bulky side groups. © 2012 Wiley Periodicals, Inc. *J Appl Polym Sci* 000: 000–000, 2012

Key words: acrylamide; association; macromonomer; salt-thickening; solution properties; viscosity

INTRODUCTION

The anionic associating water-soluble polymers, which contain a small amount of small hydrophobic monomers without long hydrophilic chains, display unique solution properties such as good resistance to shear, excellent thickening effect in pure water, salt-thickening in a narrow salt concentration range.^{1–5} In addition, the heat-thickening effect is observed for the associative polymers containing nonionic hydrophobic monomers.⁶ Such polymers have potential industrial applications in enhanced oil recovery (EOR), hydraulic fracturing, drilling fluid, drag reduction, and flocculation.^{7–10} These linear polymer chains are inevitably coiled in brine solutions because of the charge shielding throughout all polymer concentrations. Consequently, with the addition of salt, the intermolecular hydrophobically associative structures collapse, and the solution vis-

cosities are reduced sharply and are much lower than those in pure water. Moreover, these types of polymers are easily precipitated from brine solutions and the phase separation occurs at the salinities higher than 70 g L⁻¹. To enhance the associations and the apparent viscosities in brine solutions for associative polymers, we synthesized a comb-like terpolymer (PVEA) of acrylamide (AM), sodium 2-acrylamido-2-methylpropane sulfonate (NaAMPS), *p*-vinylbenzyl-terminated octylphenoxy poly(ethylene oxide) (degree of polymerization: 18) (VBPEO).¹¹ Compared with the linear associative polymers without side chains, the resistance to salt of PVEA is improved remarkably. Such polymer exhibited the salt-thickening behavior twice in a NaCl concentration range of 2–150 g L⁻¹, and high apparent viscosities (>500 mPa s, measurement condition: 30°C and 7.34 s⁻¹) in the brine solutions below 10 g L⁻¹ NaCl as well as in pure water at the polymer concentrations of 0.2 g dL⁻¹. However, for this polymer at the NaCl concentrations higher than 50 g L⁻¹, the solution viscosities are not high and are obviously lower than those in pure water throughout all polymer concentrations. Moreover, the electrostatic shielding effect from the Ca²⁺ ions is strong for PVEA, resulting in a great decrease in apparent viscosity with the addition of CaCl₂. Therefore, to meet the needs

Correspondence to: C. Zhong (zhchrong2006@yahoo.com.cn).

Contract grant sponsor: Freedom Innovation Foundation of State Key Laboratory of Oil and Gas Reservoir Geology and Exploitation; contract grant number: 024-000035.

of technical applications in oil fields, the solution viscosities are expected to be increased substantially for oil-flooding polymers used in the oil reservoirs with salinities higher than 50 g L⁻¹.

In this article, we seek to enhance the intermolecular associations and the solution viscosities in the brine solutions with NaCl concentrations higher than 50 g L⁻¹, and weaken the electrostatic shielding effect from the Ca²⁺ ions for associative water-soluble polymers. Thus, a novel macromonomer APEO: allyl-capped octylphenoxy poly(ethylene oxide) (degree of polymerization: 14) was first synthesized.¹² Then a novel polymer (PAVO) was synthesized from acrylamide, sodium 2-acrylamido-2-methylpropane sulfonate (NaAMPS), vinyl biphenyl (VP), and APEO.¹³ The solution properties of PAVO were investigated as a function of polymer and salt concentrations, temperature, shear rate, and ageing time. Consequently, the solution behavior of such polymer was completely different from those of the associating polymers without long side chains reported by literatures.^{14,15} The water-soluble copolymers with a macromonomer have been extensively studied, but most of them are used as polymer surfactants,¹⁶⁻¹⁸ hydrogels,^{19,20} carriers in drug delivery systems,²¹ etc. A few of them exhibit thickening behavior^{22,23} but the apparent viscosities of PAVO in brine solutions are much higher.

The rationale of architecture design was as follows for the PAVO polymer. It was found that the tetrapolymer of acrylamide, NaAMPS, VP and VBPEO exhibited poor resistance to salt and was precipitated by a small amount of salt because of too strong intermolecular hydrophobic associations. Thus, the phenyl group at the beginning of the side chain was not considered, and the molecular structure of APEO was determined. AM is a commonly used monomer in EOR and has good water-solubility and copolymerization activity. NaAMPS is a salt-tolerant monomer and expand polymer chains because of charge repulsion. VP can not only be used as a hydrophobic monomer but also enhance the resistance to ageing because of the presence of bulky biphenyl group.

EXPERIMENTAL

Reagents

AM was recrystallized twice from chloroform, 2-acrylamido-2-methylpropane sulfonate (AMPS) from Lubrizol Company. Vinyl biphenyl was purchased from Acros Organics Company. Tetrahydrofuran (THF) is dried with anhydrous sodium sulfate (Na₂SO₄) before use. Partially hydrolyzed polyacrylamide (HPAM) (intrinsic viscosity $[\eta]$: 54.39 dL g⁻¹, weight-average molecular weight \bar{M}_w : 2.5 × 10⁷ g mol⁻¹, hydrolysis degree: 25%, $[\eta] = 3.20 \times 10^{-4}$

$\bar{M}_w^{0.707}$) was purchased from DaQing Polymer Company in China. Other reagents were analytically pure and used without further purification.

Instrumentation

The FTIR spectrum was conducted in a NICOLET-560 FTIR spectrophotometer with a resolution capacity of 1 cm⁻¹ and the scanning number of 32. The KBr disks were prepared with the purified polymer sample. A solution of the purified APEO in CDCl₃ and a solution of the PAVO polymer in D₂O were studied with a 400 MHz Inova-400 instrument (Varian Company, USA) at the room temperature. The concentrations of the samples in CDCl₃ and D₂O were 10 mg mL⁻¹. The carbon, nitrogen, and sulfur contents of the polymers were determined with a Carlo Esra-1106 elemental analyzer (Italy). The molar percentage compositions of the PAVO polymers were calculated from the measured data using eqs. (1)–(7), where *A*, *E*, *V*, and *P* are the moles of AM, APEO, VP, and NaAMPS in 100 g of terpolymer, respectively. The coefficients are the numbers of carbon, nitrogen, and sulfur in each monomer.

$$\% C/12.01 = 3A + 45E + 14V + 7P \quad (1)$$

$$\% N/14.01 = 1A + 1P \quad (2)$$

$$\% H/1.01 = 5A + 82E + 12V + 12P \quad (3)$$

$$\% S/32.01 = 1P \quad (4)$$

$$\text{mol \% AM} = 100A/(A + E + V + P) \quad (5)$$

$$\text{mol \% APEO} = 100E/(A + E + V + P) \quad (6)$$

$$\text{mol \% VP} = 100V/(A + E + V + P) \quad (7)$$

$$\text{mol \% NaAMPS} = 100P/(A + E + V + P) \quad (8)$$

The steady shear was investigated with a Gemini 200 dynamic rheometer (Malvern Instruments Company, England) with cone-plate geometry (angle: 4° and diameter: 40 mm). The constant temperature was controlled at 45°C via a thermostatic system, and the accuracy degree was ± 0.1°C. The shear rate ranged from 0.1 to 300 s⁻¹ and the measuring time of a shear cycle was 12 min. The apparent viscosities of the polymer aqueous and brine solutions were measured at 45°C with a Brookfield DVIII R27112E viscometer at a shear rate of 7.34 s⁻¹. The intrinsic viscosities were measured with a 0.6 mm Ubbelohde capillary viscometer in a 1 mol L⁻¹ sodium nitrate solution at (30.0 ± 0.1)°C.

Synthesis of the APEO macromonomer

The APEO macromonomer was synthesized as follows. Poly(ethylene oxide) octylphenyl ether with the degree of polymerization: 14 (20 g, 0.0243 mol)

and 30 mL of dry THF were added into a 250-mL three-necked flask, and Na (0.7266 g, 0.0316 mol) was then added in the flask. After the mixture was stirred for 2 h at the room temperature under the nitrogen atmosphere, the solution of allyl chloride (1.5546 g, 0.0203 mol) in 15 mL of dry THF was added dropwise. The mixture was then heated and refluxed for 48 h. After cooling to the room temperature, the crude product solution was filtered and then concentrated by rotatory evaporation under vacuum. Finally, the crude product was purified by the column chromatography (ethyl acetate/ethanol 15 : 1, v : v) to give 7.58 g of pure product as a buff liquid (43.27% yield). $^1\text{H-NMR}$ (400 MHz, CDCl_3) shifts δ (ppm): 5.287 (d, 1H, H^a), 5.183 (d, 1H, H^b), 5.896 (dd, 1H, H^c), 4.021 (s, 2H, H^d), 3.579–3.782 (m, 52H, $\text{H}^e\text{--H}^h$), 3.837 (s, 2H, H^i), 4.113 (s, 2H, H^j), 6.831 (d, 2H, H^k), 7.130 (d, 2H, H^l), 2.551 (s, 2H, H^m), 0.600–1.576 (m, 15H, H^n). FTIR absorption peaks (cm^{-1}): C=C of $\text{CH}_2=\text{CH}$ stretch, 1643.73; =C–H of $\text{CH}_2=\text{CH}$ stretch, 3035.40; =C–H of $\text{CH}_2=\text{CH}$ bending, 944.64; aromatic C=C stretch, 1609.5, 1580.29, 1511.28; aromatic =C–H bending, 834.62; $-\text{CH}_3$, $-\text{CH}_2$ stretch, 2929.39, 2870.38; $-\text{CH}_3$, $-\text{CH}_2$ bending, 1351.88, 1459.43; $-(\text{CH}_2)_7$ bending, 751.01; C–O–C stretch, 1112.77; =C–O–C stretch, 1249.11.

Synthesis of the PAVO polymer

The PAVO polymer was prepared by the aqueous free-radical copolymerization. A 100-mL three-necked round-bottomed flask was equipped with a mechanical stirrer, a nitrogen inlet, and an outlet. AM (5.0 g, 0.0704 mol), AMPS (1.6713 g, 0.008064 mol), and sodium dodecyl sulphate (SDS) (1.3608 g) were dissolved into 41.6 mL of distilled water, and the mixture solution was then placed in the flask. NaOH was used to control the pH value of the reaction solution between 5 and 7. The mixture solution was stirred for 15 min, and APEO (0.8354 g, 9.6770×10^{-4} mol) and VP (0.2180 g, 1.2096×10^{-3} mol) were then added into the reaction flask. The flask was purged with N_2 for half an hour. The reactant solution was heated to 60°C in a tempering kettle under a nitrogen atmosphere, and 2.2 mL of $0.05 \text{ mol L}^{-1} \text{K}_2\text{S}_2\text{O}_8$ solution was then added to the solution. After the polymerization proceeded for 24 h at 60°C , the polymer mixture was diluted with 400 mL of distilled water, and 600 mL of propanol was then added with stirring to precipitate the polymer. The polymer was washed with propanol twice and extracted with propanol by the Soxhlet extractor for 2 days. Finally, the polymers were dried *in vacuo* at 50°C for 3 days.

$^1\text{H-NMR}$ (400 MHz, D_2O) shifts δ (ppm): 9H ($-\text{CH}$ of biphenyl), 7.612; 4H ($=\text{CH}$ of octylphenyl),

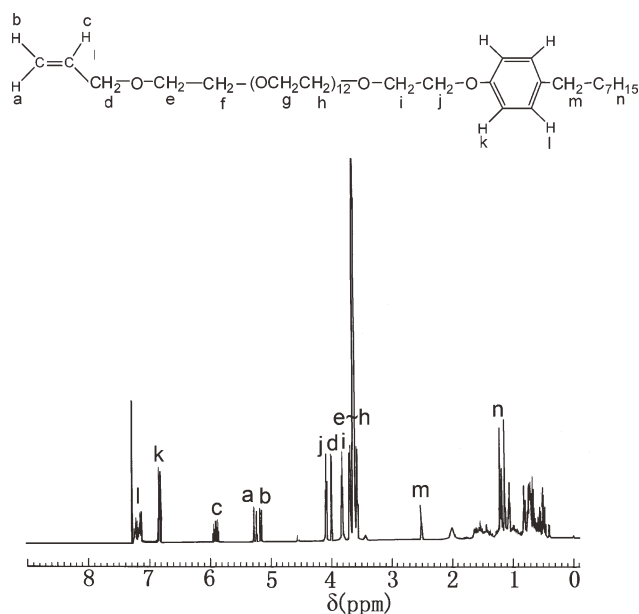


Figure 1 Schematic molecular structure and $^1\text{H-NMR}$ spectrum of APEO.

6.780; $-\text{CH}_2$ of PEO, 3.613; 17H of octyl and 2H ($-\text{CH}_2$ of APEO main chain), 1.062; 1H ($-\text{CH}$ of APEO main chain), 1.715; 6H ($-\text{CH}_3$ of AMPS side chain), 1.304; 2H ($-\text{CH}_2$ of AMPS side chain), 3.520; 2H ($-\text{CH}_2$ of NaAMPS main chain), 1.637; 1H ($-\text{CH}$ of AMPS main chain), 2.206; 2H ($-\text{CH}_2$ of AM main chain), 1.524; 1H ($-\text{CH}$ of AM main chain), 2.085; 2H ($-\text{CONH}_2$ of AM), 4.930. FTIR absorption peaks (cm^{-1}): $-\text{N-H}$ stretch, 3437.30; C=O stretch, 1643.64; $-\text{CH}_3$, $-\text{CH}_2$, $-\text{CH}$ stretch, 2872.58, 2929.39, 2777.89; $-\text{CH}_3$, $-\text{CH}_2$, $-\text{CH}$ bending, 1421.30, 1452.89, 1353.98; C=C in phenyl stretch, 1575.62; C–O of PEO stretch, 1123.23; C–O of phenol stretch, 1180.23; $-\text{SO}_3^-$: 1041.14, 605.68.

RESULTS AND DISCUSSION

Polymerization of PAVO

Composition analysis

The molecular structure of APEO was determined by $^1\text{H-NMR}$ (Fig. 1) and FTIR (Fig. 2) spectra. Both spectra confirmed the allyl group, poly(ethylene oxide) chain and octylphenyl group. Figure 1 showed the peaks ascribed to vinyl group (5.287, 5.183, and 5.896 ppm) and phenyl group (6.831 and 7.130 ppm). Figure 2 displayed the peaks of vinyl group (1643.73 and 3035.40 cm^{-1}) and phenyl group (1609.5 , 1580.29 , and 1511.28 cm^{-1}). The peaks ascribed to biphenyl group (7.612 ppm), octylphenyl group (6.780 and 1.062 ppm), EO group (3.613 ppm), amido group (4.930 ppm), and propane sulfonate group (3.520 ppm) were observed in $^1\text{H-NMR}$ spectrum of PAVO (Fig. 3). This proved the polymerization of

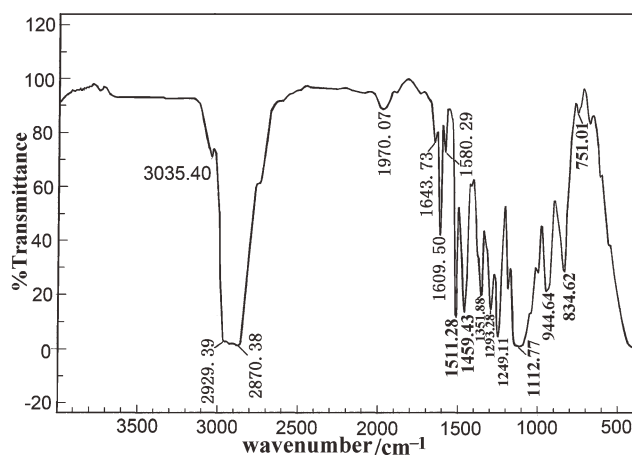


Figure 2 FTIR spectrum of APEO.

AM, NaAMPS, APEO, and VP. The polymerization conditions, viscosities, and polymer molar compositions of the PAVO samples are shown in Tables I and II. As shown in Table II, the intrinsic viscosities of PAVO were very low in comparison with HPAM used in EOR, which indicated that the molecular weights of such polymers were very low. Thus, the PAVO polymers could be easily dissolved. Furthermore, their intrinsic viscosities changed remarkably with the polymerization conditions. The apparent viscosities were significantly higher in 100 g L⁻¹ NaCl than in pure water at the polymer concentration

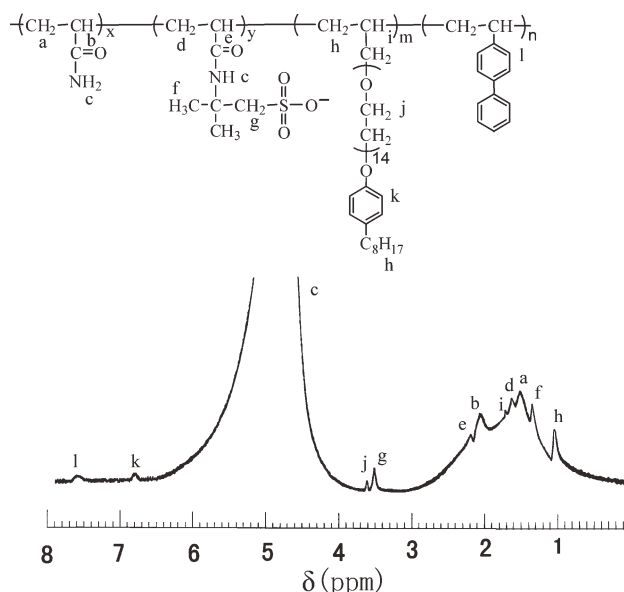


Figure 3 Schematic molecular structure and H-NMR spectrum of PAVO.

of 0.2 g dL⁻¹ for most samples. In contrast, for HPAM traditionally applied in EOR, the intrinsic viscosities are commonly higher than 15 dL g⁻¹, and the apparent viscosities reduce remarkably with increasing salt concentration at all polymer concentrations and are especially low in brine solutions with high salinities. Therefore, HPAM cannot be applied in the

TABLE I
Synthesis Conditions, Yield, and Viscosity of PAVO

Sample	Reaction conditions				Yield (%)	Apparent viscosity (mPa s) ^a	
	M1 : M2 : M3: M4 ^b	K ₂ S ₂ O ₈ ^c (mol %)	Monomers ^d (wt %)	SDS ^e (wt %)		Water	100 g L ⁻¹ NaCl
PAVO-PS0	92.0 : 6.0 : 1.0 : 1.0	0.12	15	2.0	91.2	29	36
PAVO-PS1	90.0 : 8 : 1.0 : 1.0	0.12	15	2.0	88.5	66	84
PAVO-PS2	88.0 : 10 : 1.0 : 1.0	0.12	15	2.0	85.3	85	183
PAVO-PS3	86.0 : 12 : 1.0 : 1.0	0.12	15	2.0	81.0	40	61
PAVO-IN1	88.0 : 10 : 1.0 : 1.0	0.14	15	2.0	87.1	92	317
PAVO-IN2	88.0 : 10 : 1.0 : 1.0	0.16	15	2.0	92.7	20	95
PAVO-SD1	88.0 : 10 : 1.0 : 1.0	0.14	15	1.0	44.5	33	54
PAVO-SD2	88.0 : 10 : 1.0 : 1.0	0.14	15	3.0	90.3	76	572
PAVO-SD3	88.0 : 10 : 1.0 : 1.0	0.14	15	4.0	—	—	—
PAVO-EO1	88.2 : 10 : 0.8 : 1.0	0.14	15	3.0	82.5	41	219
PAVO-EO2	87.8 : 10 : 1.2 : 1.0	0.14	15	3.0	87.8	59	824
PAVO-EO3	87.5 : 10 : 1.5 : 1.0	0.14	15	3.0	—	22	159
PAVO-VP1	88.3 : 10 : 1.2 : 0.5	0.14	15	3.0	90.6	23	7
PAVO-VP2	87.3 : 10 : 1.2 : 1.5	0.14	15	3.0	88.0	72	1210
PAVO-VP3	86.8 : 10 : 1.2 : 2.0	0.14	15	3.0	—	48	235
PAV	88.5 : 10 : 0 : 1.5	0.14	15	3.0	92.0	259	41
PAO	88.8 : 10 : 1.2 : 0	0.14	15	0	89.4	54	2

^a Polymer concentration: 0.2 g dL⁻¹; measure condition: 45°C, 7.34 s⁻¹.

^b M1, acrylamide; M2, NaAMPS; M3, APEO; M4, VP feed molar compositions.

^c Molar percentage relative to total monomer.

^d Monomers = total monomer concentration, mass percent composition in water.

^e Mass percent composition in water.

TABLE II
Feed Composition, Elemental Analysis, and Polymer Composition of PAVO

Sample	Feed composition M1 : M2 : M3: M4 ^a	Elemental composition				Polymer composition M1 : M2 : M3 : M4	Intrinsic viscosity (dL g ⁻¹)
		C (wt %)	N (wt %)	S (wt %)	H (wt %)		
PAVO-PS1	90.0 : 8 : 1.0 : 1.0	50.84	14.20	3.50	7.09	86.94 : 10.52 : 1.19 : 1.35	6.47
PAVO-PS2	88.0 : 10 : 1.0 : 1.0	50.55	13.90	3.87	7.07	85.61 : 11.87 : 1.24 : 1.28	5.31
PAVO-PS3	86.0 : 12 : 1.0 : 1.0	49.99	13.89	4.30	7.00	84.53 : 13.24 : 1.07 : 1.16	4.80
PAVO-IN1	88.0 : 10 : 1.0 : 1.0	50.53	13.66	4.04	7.06	84.72 : 12.61 : 1.30 : 1.37	4.56
PAVO-IN2	88.0 : 10 : 1.0 : 1.0	50.39	13.37	4.32	7.05	83.49 : 13.75 : 1.36 : 1.40	3.39
PAVO-SD1	88.0 : 10 : 1.0 : 1.0	50.20	15.36	3.06	7.07	90.01 : 8.60 : 0.85 : 0.54	2.84
PAVO-SD2	88.0 : 10 : 1.0 : 1.0	50.27	13.32	4.46	7.02	83.00 : 14.25 : 1.32 : 1.43	5.17
PAVO-EO1	88.2 : 10 : 0.8 : 1.0	49.88	13.96	4.38	6.97	84.38 : 13.44 : 0.97 : 1.21	5.60
PAVO-EO2	87.8 : 10 : 1.2 : 1.0	50.45	13.40	4.20	7.07	83.93 : 13.35 : 1.42 : 1.30	4.63
PAVO-VP1	88.3 : 10 : 1.2 : 0.5	49.91	13.60	4.32	7.05	84.30 : 13.60 : 1.34 : 0.76	5.48
PAVO-VP2	87.3 : 10 : 1.2 : 1.5	51.12	13.20	3.97	7.11	83.90 : 12.71 : 1.56 : 1.83	4.12
PAV	88.5 : 10 : 0 : 1.5	49.22	15.20	4.63	6.73	85.18 : 13.10 : 0 : 1.72	4.45
PAO	88.8 : 10 : 1.2 : 0	49.12	13.63	4.62	7.03	84.01 : 14.65 : 1.34 : 0	6.03

^a M1, acrylamide; M2, NaAMPS; M3, APEO; M4, VP molar compositions.

reservoirs with high salinities. The intrinsic and apparent viscosity data of PAVO also suggested that the thickening properties of such polymers should not absolutely depend on the molecular weights and be mainly determined by the supramolecular associative structures formed with the addition of salt.

The polymer molar compositions of VP, APEO, and NaAMPS were respectively higher than the monomer feed compositions (Table II). It suggested that the reaction rates of VP, APEO, and NaAMPS be higher than that of AM. AM and NaAMPS were completely dissolved in the aqueous solution, resulting in the random distribution of AM and NaAMPS in the polymer backbones. Their reactivity ratios were $r_{AM} = 0.98$ and $r_{NaAMPS} = 0.49$.²⁴ Therefore, the copolymerization tendency of NaAMPS was higher than that of AM, leading to the molar composition data of this unit in PAVO. VP and APEO were solubilized in the SDS micelles, where local concentrations of APEO and VP should be higher than that of AM in aqueous solution. This local concentration effect made the reactivity ratio of APEO and VP higher than that of AM, and could lead to the microblock segments of APEO and VP.^{6,25-27} As a result, the molar compositions of APEO in the polymer were higher than those in the feed ratios although this monomer contains long hydrophilic poly(ethylene oxide) chains and bulky benzene ring. In addition, it was found that the polymerization of APEO was indeed rapid at suitable feed amounts. Similarly, the polymerization were also rapid for *p*-vinylbenzyl-terminated alkyl poly(ethylene oxide)²⁸ and VBPEO containing the benzene rings at the beginning and the end.¹¹

Effect of NaAMPS feed amount

The nonionic acrylamide-based copolymers are difficult to dissolve into water, and the polymer chains

are coiled. Therefore, the incorporation of NaAMPS to the molecular chains can not only improve the water solubility of polymers but also facilitate the expansion of molecular chains. Accordingly, the intermolecular hydrophobic associations are easily formed. PAVO-PS2 with the NaAMPS feed amount of 10 mol % displayed the highest apparent viscosities in the aqueous solution (Fig. 4 and Table I). But for PAVO-PS2, the hydrophobically associating effect was weak, the variation of apparent viscosity with polymer concentration was not dramatic throughout the polymer concentrations, and an obvious critical association concentration (C_p^*) was not observed. The excessive NaAMPS feed amount (12 mol % NaAMPS) could result in a high charge density in polymer chains and a low-molecular weight because of the steric hindrance effect of the bulky side groups. Moreover, the too strong charge-charge repulsions could greatly weaken the intermolecular

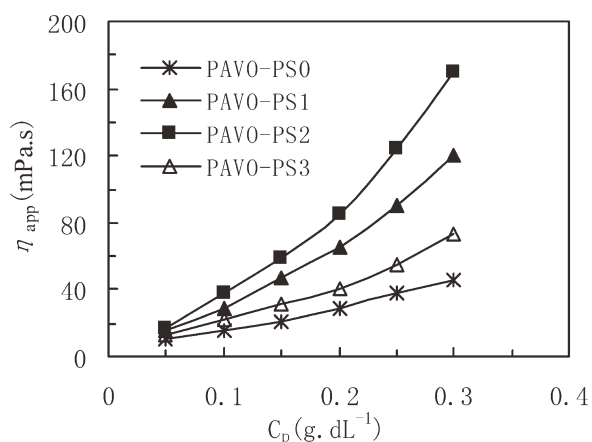


Figure 4 Effect of NaAMPS feed amount on the apparent viscosities of aqueous PAVO solutions.

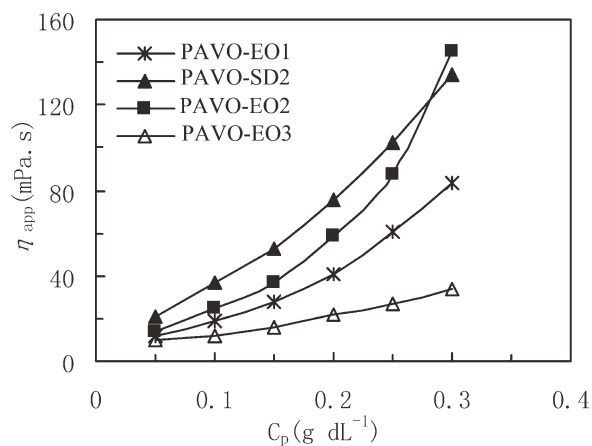


Figure 5 Effect of APEO feed amount on the apparent viscosities of aqueous PAVO solutions.

associations. Consequently, the apparent viscosity of PAVO-PS3 aqueous solution was low and slowly varied with polymer concentration.

Effect of APEO feed amount

The thickening properties of the PAVO polymers in aqueous and brine solutions are greatly influenced by the APEO feed amount (Fig. 5 and Table I). For PAVO-EO2 with the optimum APEO feed amount of 1.2 mol %, the aqueous solution showed the most obvious associative behavior, and C_p^* was 0.15 g dL⁻¹. But as the APEO feed amounts were respectively 0.8 and 1.5 mol %, the apparent viscosities of the corresponding polymers (PAVO-EO1 and PAVO-EO3) in aqueous and brine solutions were lower than those of the PAVO-EO2 and gradually varied with polymer concentration. Although the apparent viscosity in aqueous solution and the intrinsic viscosity were higher for PAVO-SD2 (APEO feed amount: 1.0 mol %), the apparent viscosity in brine solution was lower because of weaker intermolecular hydrophobic associations. For PAVO-EO2, the presence of the long side chains containing phenyl group enhanced the steric hindrance of side groups, leading to the difficult rotation of C—C bonds in main chains. Thus, the polymer chains were expanded in aqueous solution and their rigidity were remarkably enhanced. Moreover, the intermolecular hydrophobic associations were formed via the hydrophobic interactions of biphenyl groups and octylphenyl groups at the end of side chains, but the associations were not strong because of the interference of the hydrophilic PEO side chains. Consequently, C_p^* was on the high side. As the APEO feed amount was 1.5 mol %, a large amount of bubble was produced, and the steric hindrance effect of this macromonomer occurred. As a result, the tetra-polymerization became difficult, and the intrinsic viscosity and yield of the polymer were low.

Effect of VP feed amount

The apparent viscosities of the PAVO polymers in aqueous and brine solutions are not only dependent on the expanded conformation of polymer chains as determined by the APEO amount, but also on the content of small hydrophobic monomer in polymer chains. The apparent viscosity of PAVO-VP2 with the VP feed amount of 1.5 mol % was maximum in aqueous solution (Fig. 6 and Table I), and C_p^* was 0.15 g dL⁻¹. The solution viscosity changed slowly with polymer concentration for PAVO-VP1 with a low VP feed amount of 0.5 mol %. At constant surfactant and APEO concentrations, with increasing VP amount from 1.0 to 1.5 mol %, the intermolecular hydrophobic associations were strengthened above C_p^* , which resulted in an increase in solution viscosity. However, as the VP amount was increased to 2.0 mol %, the copolymerization was disturbed because of the steric hindrance of the biphenyl group, and the PAVO-VP3 with poor thickening ability was produced.

Solution properties of PAVO

Effect of polymer molecular structure

Figure 7 shows the influence of polymer concentration on the apparent viscosity for three polymers: poly(AM/NaAMPS/VP) (PAV), poly(AM/NaAMPS/APEO) (PAO), and PAVO-VP2 in aqueous solution. PAV exhibited the most prominent associative behavior in aqueous solution, and C_p^* was 0.1 g dL⁻¹, above which the apparent viscosity increased abruptly with increasing polymer concentration. However, the associative phenomenon was not observed behavior for PAO in aqueous solution, and the apparent viscosity was very low and gradually varied with polymer concentration. This indicated that the intermolecular hydrophobic associations of

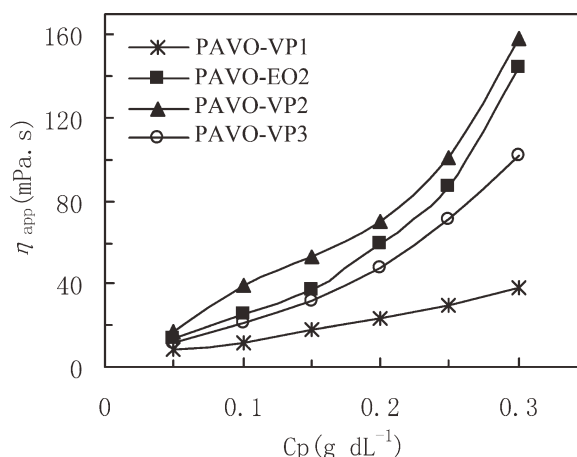


Figure 6 Effect of VP feed amount on the apparent viscosities of aqueous PAVO solutions.

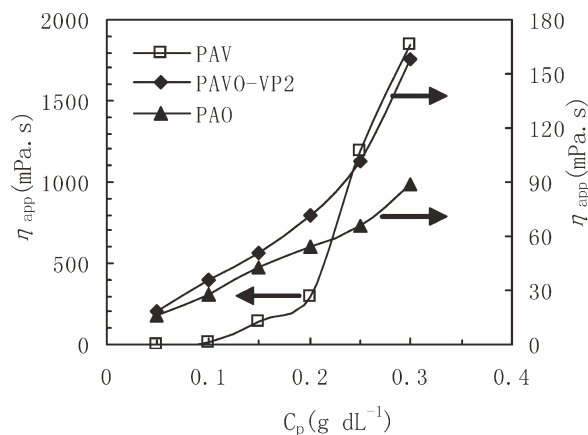


Figure 7 Effect of polymer concentration on the apparent viscosities of aqueous solutions with different polymers.

octylphenyl groups could not be formed because of the hydrophilicity of PEO side chains for this solution. For PAVO-VP2 in aqueous solution, in comparison with PAV, C_p^* (0.15 g dL^{-1}) was higher, and the apparent viscosities were much lower above 0.1 g dL^{-1} because of the low-molecular weight and weak intermolecular hydrophobic associations.

The plots of the apparent viscosity versus polymer concentration were shown in Figure 8 for PAV, PAO and PAVO-VP2 in a 100 g L^{-1} NaCl solution. The thickening behaviors of the three polymers in the brine solution were significantly different from those in aqueous solution. The PAVO-VP2 brine solution displayed the strong intermolecular associative behavior, and C_p^* decreased to 0.10 g dL^{-1} . The apparent viscosities were much higher than those in aqueous solution at the polymer concentrations higher than C_p^* . For example, as the polymer concentration was increased from 0.1 to 0.15 g dL^{-1} , the apparent viscosity increased dramatically from 2 to 173 mPa s ; the apparent viscosity was 1210 mPa.s in 0.20 g dL^{-1} PAVO-VP2. The linear PAV polymer

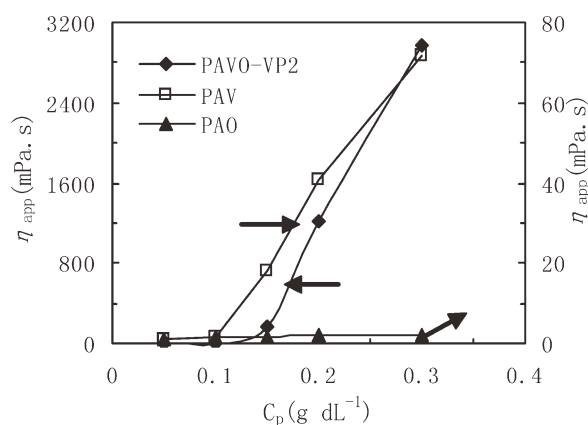


Figure 8 Effect of polymer concentration on the apparent viscosities of the 100 g L^{-1} NaCl solutions with different polymers.

without side chains also exhibited the hydrophobically associative behavior in the brine solution, and C_p^* was also 0.1 g dL^{-1} . But the viscosity was reduced remarkably with the addition of NaCl. The viscosities of the PAO brine solution were very low over all polymer concentrations.

For the PAVO-VP2 brine solution with the high NaCl concentration of 100 g L^{-1} , although the electrostatic shielding from Na^+ on the repulsive ionic interactions of $-\text{SO}_3^-$ groups may occur, the polymer chains were comparatively expanded because of the simultaneous introduction of the biphenyl group and the octylphenoxy poly(ethylene oxide) side chains. Moreover, the C—O bonds in the PEO side chains could be complex with Na^+ , which resulted in a decrease of hydrophilicity of PEO chains. This complexation enhanced remarkably the intermolecular hydrophobic associations of octylphenyl groups and biphenyl groups. Hence, a large number of polymer chains aggregated together to form reversible supramolecular microstructures, which led to high solution viscosities. In contrast to PAVO-VP2, the intermolecular hydrophobic associations of octylphenyl groups were not formed through the disturbance of the hydrophilic PEO side chains in the PAO brine solution. The linear polymer chains were greatly coiled in the 100 g L^{-1} NaCl solution for PAV, and compact aggregates were formed through the intermolecular hydrophobic associations of biphenyl groups. Consequently, the apparent viscosity reduced dramatically.

Effect of electrolytes

Figure 9 displays the variation of the apparent viscosity with NaCl concentration for the PAV, PAO, and PAVO-VP2 brine solutions. The brine solutions with 0.15 and 0.2 g dL^{-1} PAVO-VP2 showed the significant salt-thickening behavior in a wide NaCl

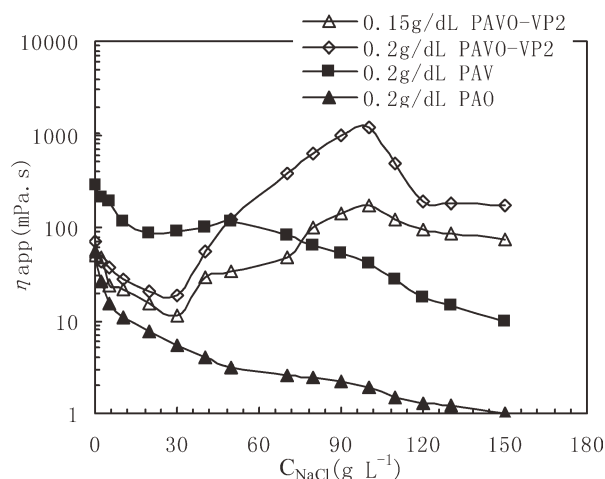


Figure 9 Effect of NaCl concentration on the apparent viscosities of the polymer brine solutions.

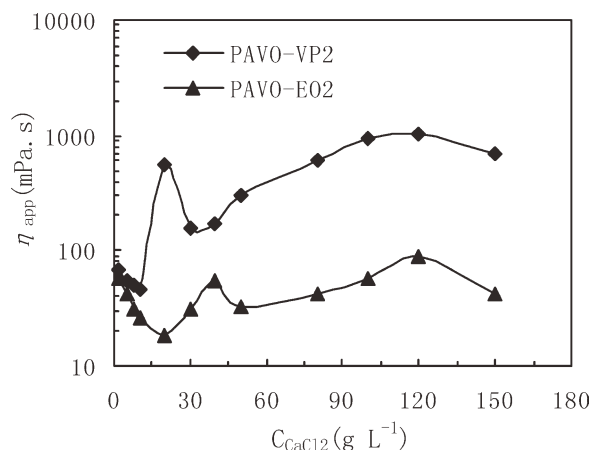


Figure 10 Effect of $CaCl_2$ concentration on the apparent viscosities of the polymer brine solutions. Polymer concentration: 0.2 g dL^{-1} .

concentration range of $30\text{--}100 \text{ g L}^{-1}$; at high NaCl concentrations of $40\text{--}150 \text{ g L}^{-1}$, their apparent viscosities were high and were much higher than those in aqueous solution. In contrast to PAVO-VP2, the brine solution of 0.2 g dL^{-1} PAV showed a salt-thickening effect in a narrow range of $20\text{--}50 \text{ g L}^{-1}$ NaCl, the maximum apparent viscosity (118 mPa s) was reached at 50 g L^{-1} NaCl. The apparent viscosities of all PAV brine solutions were lower than that in aqueous solution (289 mPa s) over NaCl concentrations. The PAO polymer showed a conventional polyelectrolyte behavior because of the shielding of charges, and the apparent viscosity reduced throughout NaCl concentrations. The apparent viscosity of the 0.2 g dL^{-1} PAVO-VP2 brine solution decreased from 42 to 19 mPa s with increasing NaCl concentration from 2 to 30 g L^{-1} . The added NaCl resulted in the charge shielding of the electrostatic repulsion of $-\text{SO}_3^-$ groups, and the intermolecular hydrophobic associations were influenced and associative structures were destroyed. However, as NaCl concentration continued increasing, the polarity of the brine solution increased; the Na^+ ions could be complex with the C—O bonds in the PEO side chains, which resulted in a decrease of hydrophilicity of the PEO chains. Consequently, the intermolecular hydrophobic associations of octylphenyl and biphenyl groups were greatly enhanced, and the salt-thickening behavior was performed in a wide range of $30\text{--}100 \text{ g L}^{-1}$ NaCl. But as NaCl concentration was further increased, the associative microstructures became more compact because of the stronger intermolecular hydrophobic associations. Hence, the apparent viscosity was reduced. But the apparent viscosity was still up to 176 mPa s at a very high NaCl concentration of 150 g L^{-1} and higher than that in aqueous solution (72 mPa s). The brine solutions behaved similarly at 0.15 g dL^{-1}

PAVO-VP2. For the PAV polymer, the linear polymer chains were greatly coiled with the addition of NaCl. Thus, the intermolecular hydrophobic associations could be disturbed remarkably in brine solution in contrast to in water. Moreover, the salt-thickening phenomenon of such polymer was only attributed to the increased solution polarity with increasing NaCl concentration, which resulted in the reinforced intermolecular hydrophobic associations. As the NaCl concentration was higher than 50 g L^{-1} , the hydrophobic microstructures became more compact, and the apparent viscosity decreased obviously.

Figure 10 displays the excellent resistance to $CaCl_2$ of the PAVO polymers in the brine solutions. Both of the 0.2 g dL^{-1} PAVO-VP2 and PAVO-E02 brine solutions exhibited the excellent salt-thickening behavior twice in a wide $CaCl_2$ concentration range of $2\text{--}150 \text{ g L}^{-1}$. The solution viscosities of both polymers were up to 1032 mPa s and 89 mPa s at 120 g L^{-1} $CaCl_2$, respectively. They were still completely dissolved in the 150 g L^{-1} $CaCl_2$ solution, and the phase separation phenomena did not appear. Compared with literatures,^{29,30} the resistance to metallic univalent and bivalent cations and the apparent viscosities in brine solutions have been improved for the PAVO polymer. For example, for the copolymer of acrylamide and allyl polyoxyethylene-12 ether with butyl-end group, the apparent viscosity is 109.39 mPa s in the brine solution with 0.222 g L^{-1} $CaCl_2$ and 0.234 g L^{-1} $MgCl_2 \cdot 6H_2O$ at a polymer concentration of 2.5 g dL^{-1} (measurement condition: 7.34 s^{-1} and 35°C). Doubtless most acrylamide-based copolymers reported were precipitated from the brine solutions with the $CaCl_2$ concentration higher than 10 g L^{-1} . The first salt-thickening mechanism induced by $CaCl_2$ could be similar to that of PAV in the NaCl solution; the second salt-thickening mechanism should be the complexation of Ca^{2+} ions with the C—O bonds in the PEO side chains, which was also similar to that induced by NaCl for PAVO-VP2. The results indicated that the phenyl-containing PEO side chains not only increased the rigidity of the polymer backbones but also behaved as the functional groups of resistance to metallic univalent and bivalent cations.

Effect of temperature

Figure 11 shows the apparent viscosities as a function of temperature for the 0.2 g dL^{-1} PAV, PAO, and PAVO-VP2 brine solutions with 100 g L^{-1} NaCl. Curve PAVO-VP2-2 was obtained by the second measurement after the measured sample was placed for 3 days. The PAVO brine solution exhibited the remarkable heat-thickening behavior in the range of $20\text{--}30^\circ\text{C}$, and then the apparent viscosity reduced sharply as temperature increased from 30 to 40°C .

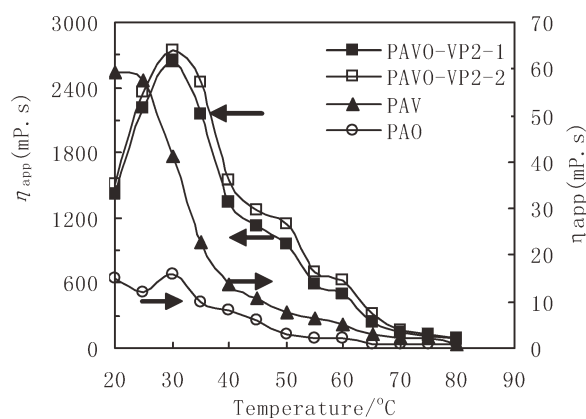


Figure 11 Effect of temperature on the apparent viscosities of the polymer brine solutions with 100 g L^{-1} NaCl. Polymer concentration: 0.2 g dL^{-1} . PAVO-VP2-1: the first measurement; PAVO-VP2-2: the second measurement.

Finally, the solution viscosity decreased gradually above 40°C (PAVO-VP2-1). In contrast, the solution viscosities of PAV and PAO almost decreased with increasing temperature because of the faster movement of the polymer chains and the destruction of hydrogen bonds. The heat-thickening effect of the PAVO brine solution within $20\text{--}30^\circ\text{C}$ should be due to the strong intermolecular hydrophobic associations of octylphenyl and biphenyl groups, which is an endothermic process of entropy increase in a certain temperature range.^{31,32} However, when the temperature was increased from 30 to 40°C , the water molecules and polymer chains moved faster. Consequently, the intermolecular hydrophobic associations were weakened, and the solution viscosity decreased. As the temperature further rose, although the faster movement of the polymer chains could interfere with the intermolecular hydrophobic associations, some hydrogen bonds formed by the C—O

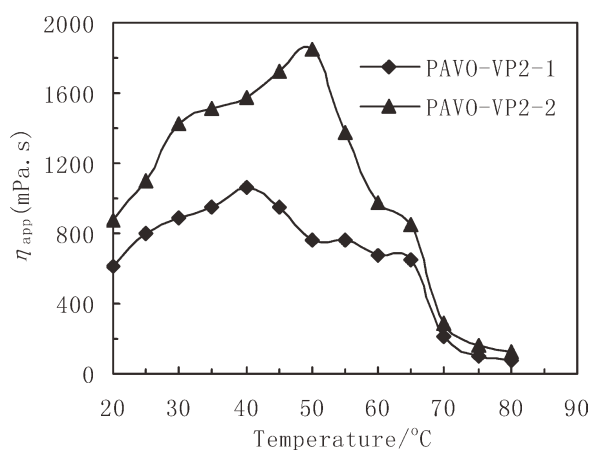


Figure 12 Effect of temperature on the apparent viscosities of the 0.2 g dL^{-1} PAVO-VP2 brine solutions with 120 g L^{-1} CaCl_2 . Polymer concentration: 0.2 g dL^{-1} . PAVO-VP2-1: the first measurement; PAVO-VP2-2: the second measurement.

bonds in PEO side chains and the water molecules should be disrupted. The hydrophilicity of PEO chains simultaneously decreased, which was favorable for the formation of the associations. Thus, the intermolecular associations were weakened more slowly, and the solution viscosities decreased slowly. The results indicated that the PEO side chains also behaved as the heat-resistant functional groups. Curve PAVO-VP2-2 showed that the polymer chains were expanded upon heating and shearing at the first measurement and that the expansion should be favorable for the intermolecular associations. This result also indicated that the intermolecular hydrophobic interactions were reversible. This reversibility is significant in polymer-flooding because polymer chains are sheared and heated continuously and the shear rate varies with sizes of pore canals in the oil reservoirs.

The apparent viscosity versus temperature is shown in Figure 12 for the 0.2 g dL^{-1} PAVO-VP2 brine solutions with 120 g L^{-1} CaCl_2 . After the measured sample was placed for 3 days, the second viscosity was much higher than the primary viscosity (Curve PAVO-VP2-2). During the first measurement (Curve PAVO-VP2-1), the PAVO-VP2 brine solution exhibited the remarkable heat-thickening behavior in the range of $20\text{--}50^\circ\text{C}$, and then the apparent viscosity decreased slowly as temperature further increased. For PAVO-VP2, the heat-thickening mechanism in the CaCl_2 solution should be also similar to that in the NaCl solution.

Effect of shear rate

Figure 13 displays the influence of shear rate on the apparent viscosity upon three consecutive shear cycles for the 0.2 g dL^{-1} PAVO-VP2 brine solution with 100 g L^{-1} NaCl. During the first shear process with an increase in shear rate, the polymer brine

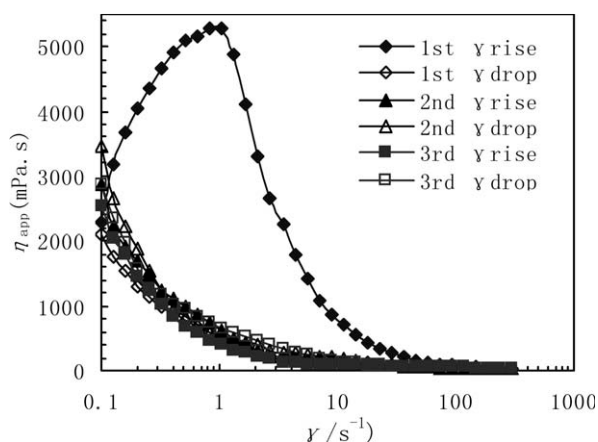


Figure 13 Effect of shear rate on the apparent viscosity of the 0.2 g dL^{-1} PAVO-VP2 brine solution with 100 g L^{-1} NaCl.

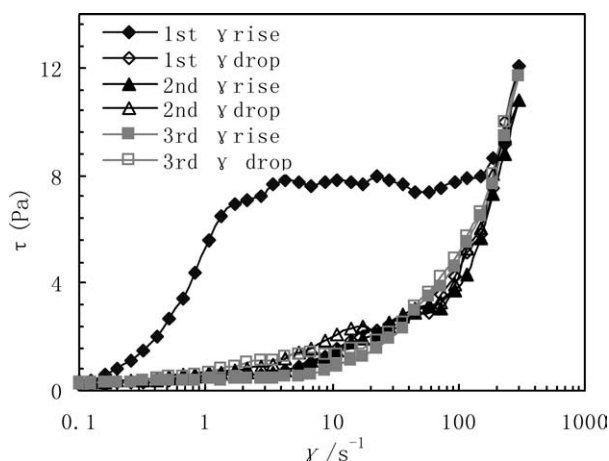


Figure 14 Effect of shear rate on the shear stress of the 0.2 g dL^{-1} PAVO-VP2 brine solution with 100 g L^{-1} NaCl.

solution showed a remarkable shear thickening behavior in a range of $0.1\text{--}1 \text{ s}^{-1}$, followed by a decrease in apparent viscosity. Finally, the solution viscosity tended to constancy above 100 s^{-1} . In the first shear reversion with a decrease in shear rate, the viscosities were almost equal to the primary ones at shear rates higher than 100 s^{-1} , and then lower than the primary ones. The viscosities in the second and third shear reversions were higher than those in the corresponding shear processes below 10 s^{-1} . This also displayed the shear thickening behavior of this brine solution. In addition, the apparent viscosity in the first shear process was also higher obviously than that in the other two shear cycles in a range of $0.1\text{--}100 \text{ s}^{-1}$. Figure 14 shows the variation of shear stress with shear rate during three shear cycles for this brine solution. For the first shear process, the shear stress increased sharply with increasing shear rate below 1.0 s^{-1} , and then did not almost change in the shear rate range of $1.0\text{--}187 \text{ s}^{-1}$. Finally, the shear stress rose dramatically at higher shear rates. For the other five shear measurements, the shear stress was almost zero below 1.0 s^{-1} , then increased slowly with an increase in shear rate within $1.0\text{--}100 \text{ s}^{-1}$, and finally increased sharply.

The proposed mechanism supported by Figures 13 and 14 is as follows: for the first shear process, the PAVO-VP2 polymer chains are expanded upon shearing below 1.0 s^{-1} . Thus, the intermolecular hydrophobic associations are strengthened, and the sizes and number of associative aggregates increase, resulting in the increase in apparent viscosity. Then these large supramolecular structures are gradually disassociated to form the smaller aggregates with increasing shear rate. Consequently, the brine solution exhibits an obvious shear thinning behavior. But the polymer chains are not stretched. This indicates that the conformation of the polymer chains is comparatively extended in brine solution. Finally,

the polymer chains were greatly expanded and orientated in fluid field above 187 s^{-1} . For the other five shear measurements, the polymer chains are not expanded and just the sizes of aggregates decrease below 1.0 s^{-1} . Then the associative aggregates are further disrupted and the polymer chains are gradually expanded within $1.0\text{--}100 \text{ s}^{-1}$. The associative structures are completely destroyed above 100 s^{-1} , resulting in low solution viscosities and high shear stresses. For six repetitious shear measurements, the solution viscosities are different below 100 s^{-1} but are almost the same at higher shear rates. This suggests that the degradation of polymer chains does not occur after repetitive shearing, and that some disrupted associative structures can not be immediately reformed at low shear rates although intermolecular hydrophobic associations are reversible.

Ageing effect

Figure 15 shows the ageing effect on 0.2 g dL^{-1} PAVO-VP2, PAV, PAO, and HPAM in 100 g L^{-1} NaCl solutions with saturated oxygen at 70°C . Presently the technically applied oil-flooding polymers are still commonly the linear superhigh-molecular-weight HPAM polymers in EOR. Thus, the ageing property of such polymer in the brine solution was also investigated. The apparent viscosity decreased slowly from 1210 to 1180 mPa s after the PAVO-VP2 brine solution was aged for 5 days. As ageing time was increased to 15 days, the apparent viscosity was still 975 mPa s and the viscosity retention ratio (ratio of reduced viscosity to primary viscosity) was 80.6% . Finally, the apparent viscosity was up to 476 mPa s (viscosity retention ratio: 39.3%) after ageing for 90 days. However, the apparent viscosities of the PAV and HPAM brine solutions reduced abruptly after ageing for 15 days. Then as ageing time was increased to 90 days, their viscosity retention ratios

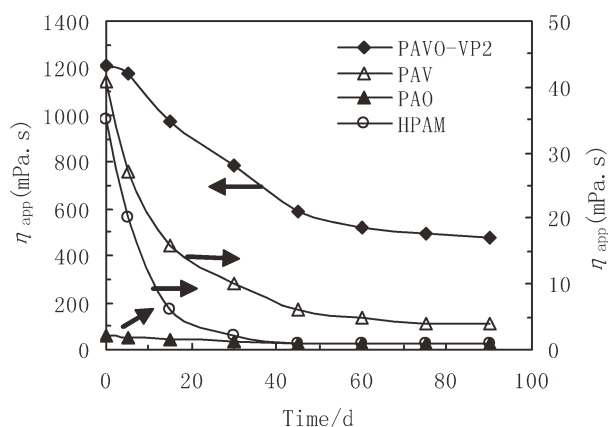


Figure 15 Influence of ageing time on the apparent viscosities of the polymer brine solutions at 70°C . Polymer concentration: 0.2 g dL^{-1} ; NaCl concentration: 100 g L^{-1} .

were only 9.7% (4 mPa s) and 2.8% (1 mPa s), respectively. These ageing data showed that the ageing resistance of PAVO was much better than those of the other three polymers at 70°C. This was due to the new polymer architecture of PAVO with the excellent thermal stability. Its rigid and bulky side groups consist of the long side chains containing phenyl group at the end, biphenyl group, and 2-amido-2-methylpropane sulphonate group. Such stable groups should effectively retard the hydrolysis of amido groups in the polymers and the oxidation degradation of the polymer chains.

CONCLUSIONS

The suitable NaAMPS feed amount could improve the water solubility of the novel polymers: poly(AM-NaAMPS-VP-APEO) (PAVO) and expand the molecular chains, which were favorable for the formation of the intermolecular hydrophobic associations. As the APEO and VP feed amounts were suitable, the steric hindrance effect of both monomers did not occur, and the local concentration effect in SDS micelles resulted in their molar polymer compositions higher than those in the feed ratios. Their simultaneous incorporation enhanced greatly the solution properties of such polymers. The hydrophilicity of PEO side chains could interfere with the hydrophobic interactions of the octylphenyl group and the biphenyl group in water for PAVO. However, the APEO macromonomer performed multifunctional effects in the brine solutions with high salinities: the intermolecular hydrophobic associations of the octylphenyl group and the biphenyl group could be greatly reinforced via the complexation of the C—O bonds in PEO side chains with the metallic univalent and bivalent cations; the side chains with phenyl group could increase the rigidity of polymer backbones and expand the polymer chains; the PEO side chains also behaved as the heat-resistant functional groups. Thus, the polymers exhibited much stronger intermolecular hydrophobic associations in the brine solutions than in water, and the apparent viscosities were much higher than in water at the polymer concentrations higher than 0.1 g dL⁻¹. Moreover, the PAVO brine solutions exhibited the significant resistance to salt, and excellent salt- and heat-thickening behaviors. The PAVO brine solution displayed good ageing resistance because of the simultaneous incorporation of three kinds of bulky side groups. The PAVO brine solution exhibited obvious shear thickening behavior at very low shear rates. This was attributed to the presence of the extended polymer chains and the remarkable enhancement of intermolecular hydrophobic associations upon shearing. However, the associative structures were greatly destroyed at higher shear rates,

resulting in a significant shear thinning behavior. The molecular chains orientated in fluid field above 100 s⁻¹ but the shear degradation of polymer chains does not occur. The repetitious shear cycles suggested that some disrupted intermolecular hydrophobic associations could not be immediately recovered although the associations were reversible.

References

- McCormick, C. L.; Kramer, M. C.; Chang, Y.; Branham, K. D.; Kathmann, E. L. *Polym Prepr* 1993, 34, 1005.
- Wei, Y. P.; Cheng, F. *Carbohydr Polym* 2007, 68, 734.
- Ma, J.; Huang, R. H.; Zhao, L.; Zhang, X. *J Appl Polym Sci* 2005, 97, 316.
- Valint, P. L., Jr.; Bock, J.; Schulz, D. N. *Polym Mater Sci Eng* 1987, 57, 482.
- Ye, L.; Luo, K. F.; Huang, R. H. *Eur Polym J* 2000, 36, 1711.
- Zhong, C. R.; Huang, R. H.; Zhang, X.; Dai, H. *J Appl Polym Sci* 2007, 103, 4027.
- Hutchinson, B. H.; McCormick, C. L. *Polymer* 1986, 27, 623.
- Taylor, K. C.; Nasr-El-Din, H. A. *J Pet Sci Eng* 1998, 19, 265.
- Dragan, S.; Ghimici, L. *Polymer* 2001, 42, 2887.
- Avoco, D.; Liu, H. Y.; Zhu, X. X. *Polymer* 2003, 44, 1081.
- Zhong, C. R.; Jiang, L. F.; Peng, X. H. *J Polym Sci Part A: Polym Chem* 2010, 48, 1241.
- Zhong, C. R.; Wang, S. G.; Peng, X. H. *Chin. Pat. CN101543747A* (2009).
- Zhong, C. R.; Wang, W.; Jiang, L. F.; Wang, S. G. *Chin. Pat. CN101463116A* (2009).
- McCormick, C. L.; Nonaka, T.; Johnson, B. C. *Polymer* 1988, 29, 731.
- Shaikh, S.; Asrof Ali, S.; Hamad, E. Z.; Abu-Sharkh, B. F. *Polym Eng Sci* 1999, 39, 1962.
- Yang, J.; Li, H. L.; Zuo, J.; An, Y. *Colloid Polym Sci* 2001, 279, 279.
- Elizabete, F. L.; Cristiane, X. S.; Gleyciane, S. P. *Polym Bull* 1997, 39, 73.
- Neugebauer, D. *Polymer* 2007, 48, 4966.
- Ingrid, W. V.; Jolanda, V. B.; Pieter, J. D.; Jan, F. J. *React Funct Polym* 2011, 71, 253.
- Chen, H. W.; Li, W. W.; Zhao, H.; Gao, J. G.; Zhang, Q. J. *J Colloid Interface Sci* 2006, 298, 991.
- Wang, K.; Xu, X.; Wang, Y. J. *Int J Pharm* 2010, 389, 130.
- Schulz, D. N.; Kaladas, J. J.; Maurer, J. J.; Bock, J.; Pace, S. J.; Schulz, W. W. *Polymer* 1987, 28, 2110.
- Tam, K. C.; Farmer, M. L.; Jenkins, R. D.; Bassett, D. R. *J Polym Sci Part B: Polym Phys* 1998, 36, 2275.
- Stahl, G. A.; Schulz, D. N. *Water-Soluble Polymers for Petroleum Recovery*; Plenum Press: New York, 1988.
- Biggs, S.; Hill, A.; Selb, J.; Caudau, F. J. *Phys Chem* 1992, 96, 1505.
- Lacik, I.; Selb, J.; Caudau, F. *Polymer* 1995, 36, 3197.
- Zhong, C. R. Study on the synthesis and properties of hydrophobically modified polyacrylamide and its associating morphology in solutions, Ph. D. Dissertation; Sichuan University: Chengdu, China, 2004.
- Ito, K.; Kazuo, T.; Hiroshige, T.; Genji, I.; Seigou, K.; Shinichi, I. *Macromolecules*, 1991, 24, 2348.
- Feng, Y. J.; Billon, L.; Grassl, B.; Bastiat, G.; Borisov, O.; Francois, J. *Polymer* 2005, 46, 9283.
- Zhou, C. J.; Yang, W. M.; Yu, Z.; Zhou, W.; Xia, Y. M.; Han, Z. W.; Wu, Q. L. *Polym Bull* 2011, 66, 407.
- McCormick, C. L.; Nonaka, T.; Johnson, C. B. *Polymer* 1988, 29, 731.
- Zhong, C. R.; Luo, P. Y. *J Polym Sci Part B: Polym Phys* 2007, 45, 826.